

RSC Publishing Faraday Discussions

**Driven Water/Ion Transport through Narrow Nanopores: a
Molecular Dynamics Perspective**

Journal:	<i>Faraday Discussions</i>
Manuscript ID	FD-ART-04-2018-000073.R1
Article Type:	Paper
Date Submitted by the Author:	30-Apr-2018
Complete List of Authors:	Coalson, Rob; University of Pittsburgh, Chemistry

SCHOLARONE™
Manuscripts

Driven Water/Ion Transport through Narrow Nanopores: a Molecular Dynamics Perspective

Author: Rob D. Coalson

Affiliation: Department of Chemistry, University of Pittsburgh, Pittsburgh, PA 15260, USA

Abstract: Atomistic Molecular Dynamics (MD) simulations provide numerous insights into the process whereby water is driven through a narrow nanopore (diameter on the order of a few water molecules) by application of hydrostatic pressure. If there are ions in the water, e.g., from dissolved salt, these may be swept along with the flowing water. If the surface of the nanopore is charged, electrostatic interaction between the surface charges and the ions as well as with partial charges on the water molecules will influence the details of the water/ion flow through the channel. Water and ion permeability depend on the geometry of the channel and the degree to which it is charged. Interesting collective features of the water molecules such as water wires that form along the pore axis and rings of water molecules that can insert into the pore perpendicular to the channel axis strongly influence the permeation process, thus emphasizing the importance of molecular level interactions in the mechanism of water and ion flow through conduits with dimensions on the molecular scale.

1) Introduction. The behavior of liquid water in confined environments is of considerable interest in many areas of scientific research [1]. Key features such as hydrogen bonding between water molecules and stabilization of ions by surrounding water shells are significantly modified when the dimensions of the confining structure reach the molecular scale. This is the situation in many biological ion channels, membrane spanning proteins with a narrow aqueous cavity through which ions such as K^+ , Na^+ , Cl^- , Ca^{+2} can pass, thus allowing them to transfer from the cytoplasm to the extracellular space [2]. Water can pass through these pores, too, and, indeed some ion channels have been specifically designed to regulate the flow of water through the cell membrane [3-7]. A particularly interesting situation arises when osmotic pressure drives water through a channel, as occurs for example in claudin channels that occupy the interstitial space between epithelial cells [8-10]. Driven water molecules can presumably drag ions (e.g., Na^+) along with them as they sweep through the channel pore.

Given the (sub)nanometer size of the species involved, it is not possible to directly observe ion channels in action experimentally. However, Molecular Dynamics (MD) simulations can do this [11]. Here we survey MD simulations of pressure driven water and ion flow through narrow model channels that can be considered as models of the claudin pore [12]. The conduits in these models are comprised of simple rigid, hydrophobic structures, essentially graphene sheets. Thus, for present purposes, we regard the study as less about pressure-driven water and ion permeation through the actual claudin channel, which is a complex and not fully understood system [10, 13], and more an analysis of physico-chemical effects that may influence the pressure-driven flow of water and ions through a narrow hydrophobic conduit lined with fixed electric charges. The work described here builds on foundations laid in previous MD studies of other model protein channels and nanotubes [14-21].

2) Simulation Methodology. In the MD simulations reported in Ref. [12], the NAMD2 program [11] with full electrostatics calculated by the particle-mesh-Ewald method was employed. All simulations were performed using the CHARMM27 force field [22] under hexagonal periodic boundary conditions at constant volume. The temperature was kept constant ($T=300$ K) using a Langevin thermostat with a damping coefficient of $5=ps$. The channel was composed of appropriately stacked and truncated graphene sheets (planar hexagonal arrays of C atoms). The TIP3P model was used for water molecules. Na^+ and Cl^- were added to the system on both sides of the channel at different concentrations. To make the simulations faster and the analysis simpler, all atoms comprising the channel were held fixed and only water molecules and ions allowed to move. The simulation system was composed of seven channels close-packed into a configuration possessing hexagonal symmetry, thus enabling multiple copies of the single-pore system to be simulated at once. Full details of the MD simulation system and protocols are given in Ref. [12].

Osmotic permeability of H_2O was estimated using the nonequilibrium MD method developed by Zhu et al. [20, 21]. A hydrostatic pressure gradient was simulated by applying a constant force in the channel axis direction to the oxygen atoms of water molecules within two 4 \AA layers which are connected through the periodic boundary condition lying in a plane outside the channel and perpendicular to its long axis; see Ref. [12] for full details.

3) MD Results: Importance of the pore geometry and pore lining charge distributions. Early models of the claudin pore suggested a structure resembling two fused cones, i.e., a double cone structure, sketched in Fig. 1 [8, 23, 24]. Carbon atoms lining the ring where the cones are fused were assigned appropriate partial charges. Application of hydrostatic pressure in the MD simulation generated a flow of water through the pore. Varying the amount of negative charge on the pore at the fusion point (which serves as a bottleneck in the structure) revealed that the rate of H₂O permeation decreased with increasing pore-lining charge over a charge range from -1.2 to -1.8 e per pore. Two interesting effects were observed that help to explain this behavior. First, Na⁺ ions, which are dragged along with water, attract to the ring of charges at the cone fusion point (center of the channel). The higher the charge of this ring, the more the Na⁺ ions tend to get stuck there, and, as a result increasingly block the flow of water through the center of the channel. Furthermore, it was found that when there were no Na⁺ ions in the channel, water molecules can form a circular structure at the junction ring, with the electropositive hydrogen atoms of the water facing the negatively lined pore and the electronegative oxygen atoms facing the pore interior, as shown in Fig. 2. This ring occludes the bottleneck region of the channel and thus slows water permeation. The ring forms more rigidly as the negative charge on the junction ring of the pore is increased.

Given that in some claudin systems it has been experimentally observed that water conduction is enhanced by an increase of negative pore lining charge [12, 23], a modified double cone structure was also considered. In this version, the junction ring in the center of the pore was expanded into a cylindrical pore section of fixed radius. In this “extended double cone” model, conical vestibules fuse to either end of the cylinder (Fig. 3). Since the fixed negative charge on the cylindrical surface is now spread out over several Angstroms, water molecules no longer form a circular structure inside the cylinder that would obstruct water/ion flow, and Na⁺ ions can more easily interact with the negative charge lining the cylinder pore by spreading out along the pore surface. Also, in the extended double cone geometry, water wires form along the pore axis, as discussed in detail below, further facilitating the flow of water through it. For a cylinder length of 10-16 Å, water flux does indeed increase with the amount of negative charge lining the cylinder pore surface over a significant range of pore charge. At very high pore charge, the water flux vs. pore lining charge curve enters a turnover region, beyond which the water flux decreases with increasing pore charge. The water wires that extend through the pore (as described in detail below) are disrupted in the regime of very high pore surface charge by the increased electrostatic interactions of the pore charges with Na⁺ and partial charges on the H₂O molecules.

The computed flux vs. hydrostatic pressure curve was found to be nearly linear, allowing for the extraction of the permeability coefficient for water flow through the pore, as prescribed by the formula $p_f = \frac{j}{\Delta P} k_B T$, where p_f is the desired osmotic permeability coefficient per pore, j is the net water flux through a single pore, ΔP is the applied hydrostatic pressure, k_B is Boltzmann’s constant and T is the absolute temperature [20, 21]. In the MD simulations surveyed here, the applied pressures are considerably higher than in electrophysiology experiments, which use osmotic pressure (induced by the introduction of appropriate osmolyte molecules on one side of the membrane). Furthermore, the ratio of H₂O molecules/Na⁺ ions flowing through the pore obtained from the simulations stays relatively constant

under significant variations of fixed pore charge and salt concentration, having a value of ~ 220 , which compares favorably to experimental estimates for the claudin channel of ~ 100 [12]. Water permeability values extracted from these MD simulations fall in the range of ca. $5 \times 10^{-13} - 1 \times 10^{-12} \text{ cm}^3/\text{s}$. By way of comparison, the experimentally measured value of water permeability in the aquaporin protein channel is ca. $10^{-13} \text{ cm}^3/\text{s}$ [3].

From a conceptual perspective, it is of interest to reverse the charge signs in the system, i.e., consider an extended double cone model where the pore is lined with positive fixed charge, thus attracting negative (Cl^-) ions into the channel along with water molecules. It might be expected that the overall implications of the positively lined pore would be similar to those of its negatively charged analog, and indeed the rate of water permeation at the same hydrostatic pressure was found to be quite similar in the two cases.

Not surprisingly, the water flow rate through the extended cone channel was found to increase with the diameter D of the cylindrical pore. The increase is not linear with respect to pore diameter, but instead occurs in quasi-quantized jumps. These jumps correlate directly with formation of multiple water wires along the pore axis, as illustrated in Fig. 4. Below $D=3.8 \text{ \AA}$, no water wires form and the water permeation rate is low. Between $D=3.8-5.0 \text{ \AA}$, one water wire forms. At $D=5.5 \text{ \AA}$, two and three water wires form, with a corresponding jump in water conduction. At $D=6.7 \text{ \AA}$, four water wires were observed. When $D=8 \text{ \AA}$, many water wires were observed.

In the MD simulations, for a given pore diameter and fixed pore lining charge, the ratio of water molecules to Na^+ ions that transport through the pore was found to be nearly constant over a significant range of applied hydrostatic pressure, as noted above. When the pore diameter is reduced (all other system parameters being equal), the ratio of H_2O molecule/ Na^+ ion transport increases, due primarily to the increased attraction of the Na^+ ions to the pore, which reduces Na^+ flux more than H_2O flux.

Another way to drive ions through the pore is to apply an electric field along the channel axis [25]. This phenomenon underlies much of ion channel biophysics, where such electric fields can be generated by a slight imbalance of ions on one side of the embedding membrane vs. the other, or by introducing external electrodes into the system [2]. Here we consider a simple case where there is no applied hydrostatic pressure and the fixed (negative) charge on the channel is low. In this case, owing to the hydrophobic character of this graphene-based channel, water tends to be expelled from the pore. When the Na^+ ions are subjected to a constant force along the channel direction (mimicking the

application of a static electric field), they are observed to migrate through the channel, dragging a cloud of 12-20 waters with each ion (cf. Fig. 5), with the average number increasing as the charge on the pore increases. These ion-water cloud complexes exhibit a relatively long (multi nanosecond) residence time inside the pore.

4) Conclusions: The flow of water through nanopores under the influence of applied hydrostatic pressure is interesting for numerous reasons. First and foremost, there is the challenge to understand the mechanism of externally driven water flow through conduits so narrow that the molecular granularity of the water molecules and their chemical interactions with the pore wall strongly influence the transport. When there are ions in the water solution, these ions will in general be swept along by water that is driven by the application of hydrostatic pressure. The interaction of the ions with charged molecular groups that line the inside of the pore can influence the flow of ions through the pore, which in turn influences water permeation.

From an experimental perspective, synthetic nanotubes, often constructed from carbon nanotubes, are interesting systems for testing conceptual understanding, and have potential technological applications as nanoscale chemical detection devices and in nano-electronics and nano-optics [26]. In addition, biological ion channels that serve as conduits for water flow from one side to the other of a cell membrane under the influence of osmotic pressure play a critical role in physiology (e.g., nephrology [8, 9]). While the structures of these biological ion channels are complicated (certainly much more complex than the rigid graphene sheet based computational model considered in this paper) and not fully understood at present, they function on the same physico-chemical principles that govern the transport behavior of water and ions through carbon nanotubes and, indeed, through the related channel models considered herein.

MD studies of these model channels have revealed interesting consequences of channel geometry and the distribution of permanent charge along the channel pore surface [12]. In a double-cone model (Fig. 1) where the cones fuse in a central ring of negatively charged atoms, this ring acts as a gate that prevents water and Na^+ ions from passing through it to a greater extent as the charge on the ring increases. This effect was traced to two interesting molecular level features. First, Na^+ ions become more strongly bound at the fixed charge ring, and, second, under certain conditions a circular water structure inserts itself into the ring (Fig. 2) due to electrostatic interactions of the partial charges on the water molecules with the negative fixed charges on the ring. Both features tend to clog the pore at the bottleneck, thus hindering flow of water and ions through it.

If the fusion ring in the double cone model is replaced by a cylinder of length $\sim 10 \text{ \AA}$, i.e., in the “extended double cone” model (Fig. 3), the sharp bottleneck feature is removed. Na^+ ions that are attracted to the negative charge along the pore lining ring can spread out along the cylinder and thus be

accommodated in the channel more easily than in the fused double cone model. Furthermore, inserted water rings (*vide supra*) are not observed in this channel geometry. This results in an increase in the current of ions and water as fixed charge on the pore surface is increased.

Focusing again on the extended double cone model, the radius of the cylindrical section of the channel was varied. Increasing the cylinder radius naturally led to a higher rate of transport of water and Na^+ through the channel. The larger the channel radius the more water wires that could extend through it. As the threshold radius for inclusion of another water wire was passed, the flow rate jumped in a quasi-quantized fashion. Finally, an initial examination was carried out on the flow induced by force on the Na^+ ions, as could be experimentally realized by applying static electric field along the channel axis. In this case, a water cloud was found to be dragged along with the Na^+ ions through the pore. This type of electroosmotic effect, which is well studied in microfluidics systems [27], has been relatively less studied in the case of narrow carbon nanotubes and biological ion channels.

Clearly, even in a simple model of a membrane spanning nano-channel with a radius of the order of a few water molecule diameters, the range of mechanisms that underlie coupled water and ion transport under the influence of applied hydrostatic pressure is extensive. Further study will be required to attain a full understanding of these processes and how to exploit them for nanotechnology applications.

Acknowledgments: This work was supported by NSF grant CHE1464551. Extensive discussions with Drs. R. Laghaei and A. Yu as well as their contributions to the research reported in Ref. [12] are gratefully acknowledged.

References:

1. Schoch, R.B., J. Han, and P. Renaud, *Transport Phenomena in Nanofluidics*. Rev. Mod. Phys., 2008. **80**: p. 839-883.
2. Hille, B., *Ion channels of excitable membranes*. 3rd ed. ed. 2001, Sunderland: Sinauer Associates, Inc.
3. Mamonov, A.B., R.D. Coalson, M.L. zeidel, and J.C. Mathai, *Water and Deuterium Oxide Permeability through Aquaporin 1: MD Predictions and Experimental Verification*. J. Gen. Physiol., 2007. **130**: p. 111-116.
4. Murata, K., K. Mitsuoka, T. Hirai, T. Walz, P. Agre, J.B. Hyemann, A. Engel, and Y. Fujiyoshi, *Structural Determinants of Water Permeation through Aquaporin-1*. Nature, 2000. **407**: p. 599-605.
5. Nielsen, S., J. Frokiaer, D. Marples, T.H. Kwon, P. Agre, and M.A. Knepper, *Aquaporins in the Kidney: From Molecules to Medicine*. Physiol. Rev., 2002. **82**: p. 205-244.
6. Sui, H., B.G. Han, J.K. Lee, P. Walian, and B.K. Jap, *Structural Basis of Water-Specific Transport through the AQP1 Water Channel*. Nature, 2001. **414**: p. 872-878.
7. Tajkhorshid, E., P. Nollert, M.O. Jensen, L.J. Miercke, O.C. J., R.M. Stroud, and K. Schulten, *Control of the Selectivity of the Aquaporin Water Channel Family by Global Orientational Tuning*. Science, 2002. **296**: p. 525-530.
8. Gunzel, D. and A.S.L. Yu, *Claudins and the Modulation of Tight Junction Permeability*. Physiol. Rev., 2013. **93**: p. 525-569.
9. Rosenthal, R., S. Milatz, S.M. Krug, B. Oelrich, J.D. Schulzke, S. Amasheh, D. Gunzel, and M. Fromm, *Claudin-2, a component of the tight junction, forms a paracellular water channel*. J Cell Sci, 2010. **123**(Pt 11): p. 1913-21.
10. Suzuki, H., T. Nishizawa, K. Tani, Y. Yamazaki, A. Tamura, R. Ishitani, N. Dohmae, S. Tsukita, O. Nureki, and Y. Fujiyoshi, *Crystal Structure of a Claudin Provides Insight Into the Architecture of Tight Junctions*. Science, 2014. **344**: p. 304-307.
11. Phillips, J.C., R. Braun, W. Wang, J. Gumbart, E. Tajkhorshid, E. Villa, C. C., R.D. Skeel, L. Kale, and S. K., *Scalable Molecular Dynamics with NAMD*. J. Comput. Chem., 2005. **26**: p. 1781-1802.
12. Laghaei, R., A.S.L. Yu, and R.D. Coalson, *Water and ion permeability of a claudin model: A computational study*. Proteins (Structure, Function, Bioinformatics), 2016. **84**: p. 305-315.
13. Suzuki, H., K. Tani, A. Tamura, S. Tsukita, and Y. Fujiyoshi, *Model for the Architecture of Claudin-Based Paracellular Ion Channels Through Tight Junctions*. J. Mol. Biol., 2015. **427**: p. 291-297.
14. Köfinger, J., G. Hummer, and C. Dellago, *A One-Dimensional Dipole Lattice Model for Water in Narrow Nanopores*. J. Chem. Phys., 2009. **130**: p. 154110:1-16.
15. Köfinger, J., G. Hummer, and C. Dellago, *Single-File Water in Nanopores*. Phys. Chem. Chem. Phys., 2011. **13**: p. 15403-15417.
16. Zhu, F. and G. Hummer, *Drying Transition in the Hydrophobic Gate of the GLIC Channel Blocks Ion Conduction*. Biophys. J., 2012. **103**: p. 219-227.
17. Hummer, G., J.C. Rasaiah, and J.P. Noworyta, *Water Conduction through the Hydrophobic Channel of a Carbon Nanotube*. Nature, 2001. **414**: p. 188-190.
18. Beckstein, O. and M.S.P. Sansom, *Liquid-Vapor Oscillations of Water in Hydrophobic Nanopores*. Proc. Natl. Acad. Sci., 2003. **100**: p. 7063-7068.
19. Beckstein, O. and M.S.P. Sansom, *The Influence of Geometry, Surface Character, and Flexibility on the Permeation of Ions and Water Through Biological Pores*. Phys. Biol., 2004. **1**: p. 42-52.

20. Zhu, F. and K. Schulten, *Water and Proton Conduction Through Carbon Nanotubes as Models for Biological Channels*. *Biophys. J.*, 2003. **85**: p. 236-244.
21. Zhu, F., E. Tajkhorshid, and K. Schulten, *Theory and Simulation of Water Permeation in Aquaporin-1*. *Biophys. J.*, 2004. **86**: p. 50-57.
22. MacKerell, A.D., C.L. Brooks, L. Nilsson, B. Roux, Y. Won, and M. Karplus, *Charmm: The Energy Function and Its Parameterization with an Overview of the Program*. Vol. 1. 1998, Chichester, U. K.: John Wiley & Sons.
23. Yu, A.S., M.H. Cheng, S. Angelow, D. Gunzel, S.A. Kanzawa, E.E. Schneeberger, M. Fromm, and R.D. Coalson, *Molecular Basis for Cation Selectivity in Claudin-2-Based Paracellular Pores: Identification of an Electrostatic Interaction Site*. *J. Gen. Phys.*, 2009. **133**: p. 111-127.
24. Yu, A.S.L., M.H. Cheng, and R.D. Coalson, *Calcium Inhibits Paracellular Sodium Conductance Through Claudin-2 by Competitive Binding*. *J. Biol. Chem.*, 2010. **285**: p. 37060-37069.
25. Mao, M., S. Ghosal, and G. Hu, *Hydrodynamic Flow in the Vicinity of a Nanopore Induced by an Applied Voltage*. *Nanotech.*, 2013. **24**: p. 245202.
26. Hu, G.I., M. Mao, and S. Ghosal, *Ion Transport Through a Graphene Nanopore*. *Nanotech.*, 2012. **23**: p. 395501.
27. Ghosal, S., *Fluid Mechanics of Electroosmotic Flow and Its Effect on Band Broadening in Capillary Electrophoresis*. *Electroph.*, 2004. **25**: p. 214-228.

Figures:

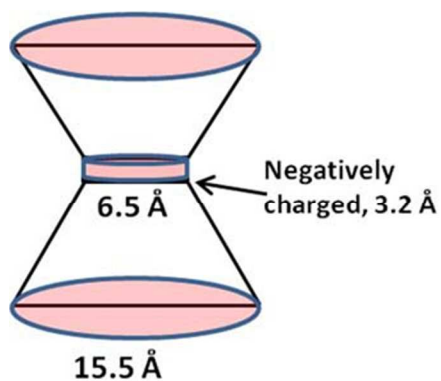


Fig. 1. Double cone channel model. A single channel is modeled as a fused double cone with 6.5 Å diameter at the narrowest part of the pore. The outer diameter is 15.5 Å. Six negatively charged spheres are placed at the narrowest position of the channel in a cylindrical band of width 3.2 Å. (Reproduced with permission from Ref. [12].)

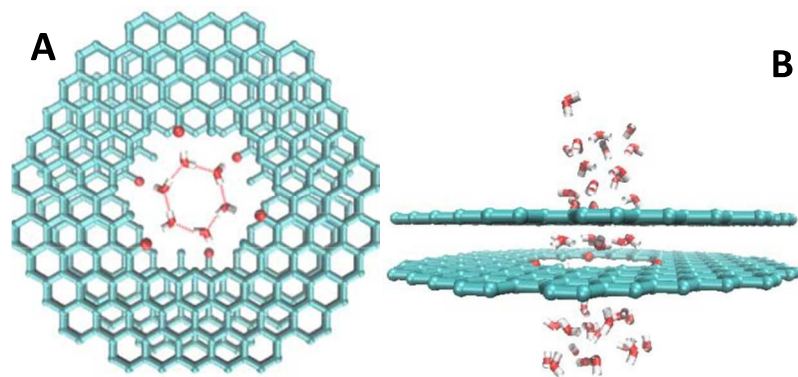


Fig. 2. Example of how water molecules link via hydrogen bonding (red dashed lines) into a circle at the center of the pore when a sodium ion is not occupying this site. The charged carbons are shown as small red circles on the edges of graphene sheets (cyan). Panel A looks down from above the channel entrance; panel B presents a side view. (Reproduced with permission from Ref. [12].)

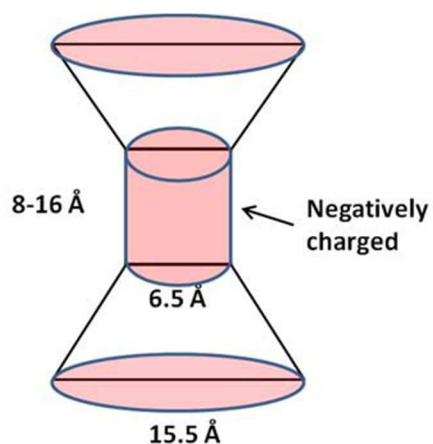


Fig. 3. Double-cone with extended selectivity filter model. The pore-lining charge is evenly distributed over a 8-16 Å long cylindrical portion of the pore. The outer diameter of the cone is 15.5 Å. (Reproduced with permission from Ref. [12].)

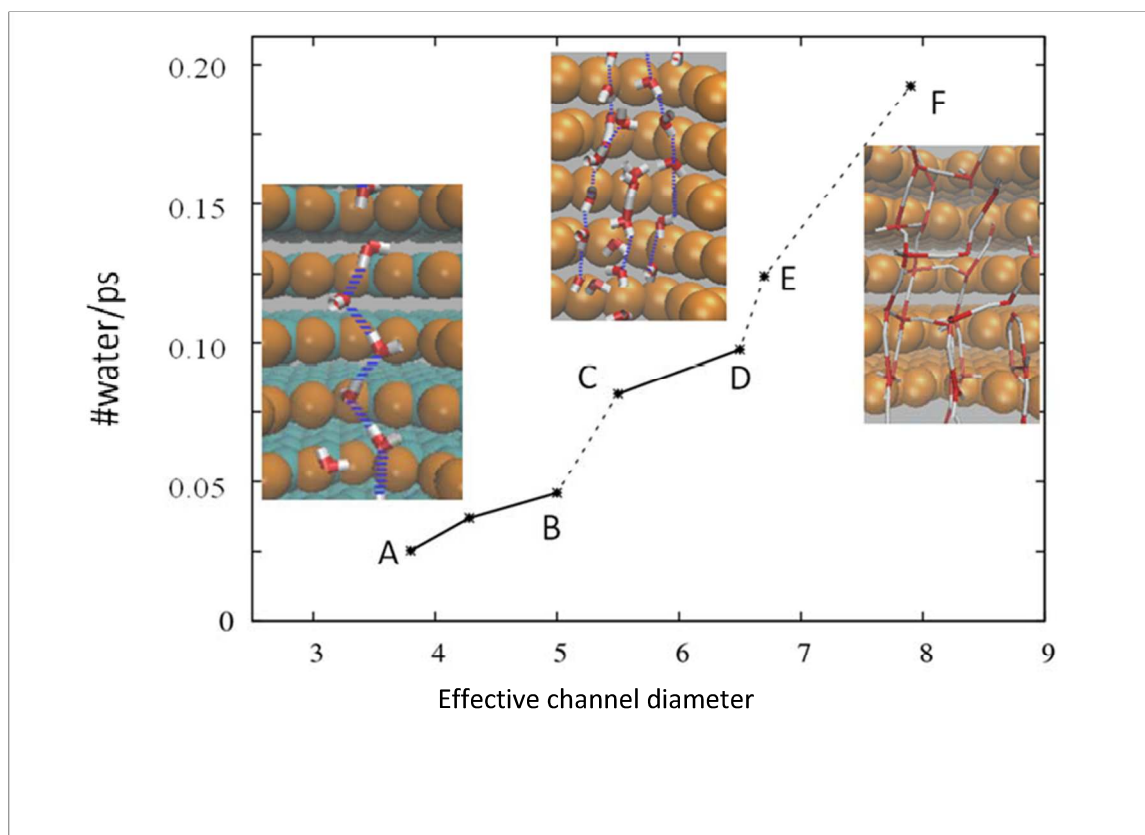


Fig. 4. Rate of water molecules that pass through pores with different effective diameters and its relation to the number of water wires that form inside the pore. Quantized jumps in the water permeability occur as the channel diameter increases, corresponding to the sequential onset of additional water wires. The applied force is 0.10 kcal/mol/Å on a 20 Å thick water layer. (Reproduced with permission from Ref. [12].)

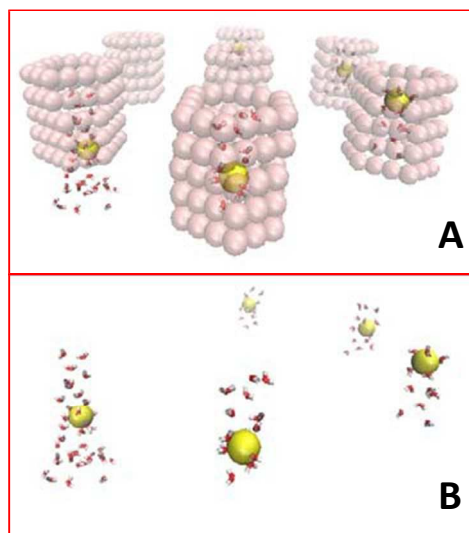


Fig. 5. A) Na^+ (yellow spheres) surrounded by water inside the 7 pores that comprise the simulation system (pink transparent spheres represent the narrowest section of each pore). Force is applied only on Na^+ ions. Each pore has a total charge of $-1.2 e$. B) The same snapshot as A, except that the pore-lining atoms have been hidden to highlight the water structure inside the pore. (Reproduced with permission from Ref. [12].)